Ground-state properties and superfluidity of two- and quasi-two-dimensional solid ^{4}He

Ground-state properties and superfluidity of two- and quasi-two-dimensional solid ^{4}He

C Cazorla[1], G E Astrakharchik[2], J Casulleras[2] and J Boronat[2]

[1] Department of Chemistry, University College London, London WC1H 0AH, UK
[2] Departament de Física i Enginyeria Nuclear, Campus Nord B4-B5, Universitat Politècnica de Catalunya, E-08034 Barcelona, Spain

E-mail: c.silva@ucl.ac.uk

Abstract
In a recent study we have reported a new type of trial wavefunction symmetric under the exchange of particles, which is able to describe a supersolid phase. In this work, we use the diffusion Monte Carlo method and this model wavefunction to study the properties of solid ^{4}He in two- and quasi-two-dimensional geometries. In the purely two-dimensional (2D) case, we obtain results for the total ground-state energy and freezing and melting densities which are in good agreement with previous exact Monte Carlo calculations performed with a slightly different interatomic potential model. We calculate the value of the zero-temperature superfluid fraction ρ_s/ρ of 2D solid ^{4}He and find that it is negligible in all the considered cases, similarly to what is obtained in the perfect (free of defects) three-dimensional crystal using the same computational approach. Interestingly, by allowing the atoms to move locally in the direction perpendicular to the plane where they are confined to zero-point oscillations (quasi-2D crystal), we observe the emergence of a finite superfluid density that coexists with the periodicity of the system.

1. Introduction

Quantum crystals are characterized by unusually large atomic kinetic energy, Lindemann ratio and non-negligible anharmonicity even at low temperatures and high pressures [1, 2]. The counterintuitive possibility of simultaneous solid order and superfluidity in solid ^{4}He, the most representative of quantum crystals, has long attracted the interest of both theoreticians and experimentalists. After several unfruitful experiments to detect superfluid signals in solid ^{4}He, Kim and Chan reported few years ago the first evidence of non-classical rotational inertia (NCRI) both in confined environment [3] and in bulk [4]. From then on, several other experimental groups (up to five, so far) have observed NCRI using different samples containing small or ultra-small ^{3}He concentrations, in a simple crystal or in a polycrystal, and using several annealing schemes [5]. There is almost overall agreement of all the data concerning the onset temperature $T_0 = 75$–150 mK at which the superfluid fraction becomes zero, the lowest value corresponding to ultra-pure samples (only 1 ppb ^{3}He). However, the experimental values of the superfluid density reported so far change by more than

one order of magnitude ($\rho_s/\rho \simeq 0.03$–0.5%) depending on the purity, annealing conditions in which the crystal is grown, etc. Such high dispersion suggests that the superfluid signal observed in solid ^{4}He is probably due to the presence of some defects in the crystal, which could be of a different nature: dislocations, vacancies or grain boundaries [6].

On the theoretical side, path integral Monte Carlo (PIMC) calculations performed at low temperatures (down to 0.1 K) show that perfect commensurate ^{4}He crystal possesses neither finite superfluid fraction [7] nor condensate fraction [8]. Only non-zero ρ_s/ρ has been estimated in the presence of disorder introduced in the form of a glassy phase [9] and of defects like dislocation lines [10] and vacancies [11]. Moreover, our recent calculations based on the diffusion Monte Carlo (DMC) method show negligible superfluid fraction of perfect bulk solid ^{4}He at strictly zero temperature [11]. These DMC calculations have been performed using a new model of a trial wavefunction which allows simultaneously for spatial solid order and Bose–Einstein symmetry and with the benefit of a simple use for importance sampling. It has been shown that the energetic and structural properties of solid ^{4}He can be

reproduced very accurately with this trial wavefunction model when it is used for importance sampling in the diffusion Monte Carlo method.

In this work, we extend our study of solid helium to purely two- and quasi-two-dimensional geometries relying upon similar computational approaches to the ones used in [11, 12]. The motivation for carrying out the present study is four-fold. First, relevance of quantum fluctuations is generally enhanced in systems of reduced dimensionality hence possible signatures of superfluidity may be detected more easily. Second, from a computational point of view low-dimensional systems are reasonably affordable so one can explore wide thermodynamic ranges on them. Third, in a recent study [12] of strictly two-dimensional solid H_2 we have shown that when the density of particles is reduced down to practically the spinodal point, a finite superfluid fraction is observed to appear in the film; in this work we carry out similar investigations on solid ^{4}He (that is in the metastable regime) in order to unravel possible connections between the density of particles and the superfluid fraction. And fourth, theoretical predictions on low-dimensional model systems can provide valuable understanding of the experimental realization of solid helium confined to restricted geometries and also an interpretation of supersolid signatures in general [13–16].

There is previous work done on the estimation of the ground-state properties of strictly 2D solid ^{4}He. Many years ago, Whitlock *et al* [17] performed a systematic study of the energetic and structural properties of this system based on the Green's function Monte Carlo approach (GFMC). More recently, Gordillo *et al* [18] estimated the phase diagram of two-dimensional ^{4}He over a range of temperatures and coverages using PIMC calculations. Also, various authors have reported on the melting transition and dynamical properties of helium films using variational and *exact* ground-state methods [19, 20]. Interestingly, Vitali *et al* [20] have investigated the existence of off-diagonal long range order (ODLRO) in 2D solid ^{4}He using the zero-temperature version of PIMC adapted to the shadow wavefunction formalism, the so-called shadow path integral ground-state method (SPIGS). In the present paper, we provide comparison with respect to the results reported in these previous works and present new predictions as well. In particular, we report on direct estimations of the superfluid fraction in 2D solid helium and its dependence on the density of particles. We also analyze the superfluid behavior of a quasi-2D crystal, i.e. an ensemble of He atoms confined within a plane but allowed to explore the out-of-plane direction locally, and assess its dependence on the density of particles and degree of confinement. In the quasi-2D case, we observe the presence of a superfluid signal which coexists with the periodicity of the system.

The remainder of the paper is organized as follows. In section 2, we summarize the basics of the DMC method and describe the symmetrized trial wavefunction model used throughout this work. Next, we report results for the ground-state properties of 2D and quasi-2D solid helium. Finally, we present some discussions and the conclusions in section 4.

2. Method and trial wavefunction

We study the ground-state of 2D solid ^{4}He by means of the DMC method and Hamiltonian $H = -\hbar^2/2m_{\text{He}} \sum_{i=1}^{N} \nabla_i^2 + \sum_{i<j}^{N} V(r_{ij})$, with N being the number of particles. The He–He atomic interaction is modeled with the semi-empirical pairwise potential due to Aziz *et al* [21] (heretofore referred to as Aziz II). The DMC method solves stochastically the imaginary time (τ) Schrödinger equation, providing essentially exact results for the ground-state energy and diagonal properties of bosonic systems within controllable statistical errors. For $\tau \to \infty$, sets of configurations (walkers) $\mathbf{R}_i \equiv \{\mathbf{r}_1, \ldots, \mathbf{r}_N\}$ generated with DMC render the probability distribution function ($\Psi_0 \Psi$), where Ψ_0 and Ψ are the ground-state wavefunction and trial wavefunction for importance sampling, respectively. The short-time Green's function approximation that we use, and according to which the walkers evolve, is accurate up to order $(\Delta\tau)^3$; technical parameters in the calculations, such as the mean population of walkers (=400) and time step $\Delta\tau$ (=5×10^{-4} K^{-1}), have been adjusted in order to eliminate possible bias in the total energy per particle to less than 0.02 K/atom [22, 23].

Customarily, structural and energetic properties of solid ^{4}He are explored with the Nosanow–Jastrow (NJ) trial wavefunction

$$\Psi_{\text{NJ}}(\mathbf{r}_1, \ldots, \mathbf{r}_N) = \prod_{i<j}^{N} f(r_{ij}) \prod_{i,I=1}^{N} g(r_{iI}) = \psi_J \psi_L, \quad (1)$$

where N is the number of particles (in this work we consider commensurate crystals only so N is also equal to the number of lattice sites), $f(r)$ being a two-body correlation factor accounting for atomic correlations and $g(r)$ a one-body localization factor which accounts for the periodicity in the system by linking every particle to a particular lattice site of a perfect crystal structure. The wavefunction Ψ_{NJ} leads to an excellent description of the equation of state and structural properties of quantum solids [24] but it cannot be used to estimate properties which are directly related to the quantum statistics. The reason for this is that Ψ_{NJ} is not symmetric upon the exchange of particles and it misses the quantum statistics of the system.

In a recent work [11], we have introduced a new type of wavefunction, Ψ_{SNJ}, which reproduces crystalline order and fulfils Bose–Einstein symmetry requirements simultaneously. This model wavefunction is expressed as

$$\Psi_{\text{SNJ}}(\mathbf{r}_1, \ldots, \mathbf{r}_N) = \prod_{i<j}^{N} f(r_{ij}) \prod_{J=1}^{N} \left(\sum_{i=1}^{N} g(r_{iJ}) \right), \quad (2)$$

where the product in the second term runs over lattice site indexes. Compact and manageable analytical expressions for the drift velocity and kinetic energy derive from equation (2), so Ψ_{SNJ} is very well suited for implementation in DMC codes. This model has proved to perform excellently in the description of bulk solid ^{4}He and also p-H_2 in two dimensions [12]. The key point in Ψ_{SNJ} is that the localization factor (second term in equation (2)) is constructed in such a way that voids originated

by multiple occupancy of the same site are penalized (this feature will be illustrated in brief by a simple example).

A similar model, Ψ_{LNJ}, has been proposed recently by Zhai and Wu [25], which is

$$\Psi_{\text{LNJ}}(\mathbf{r}_1, \ldots, \mathbf{r}_N) = \prod_{i<j}^{N} f(r_{ij}) \prod_{i=1}^{N} \left(\sum_{J=1}^{N} g(r_{iJ}) \right) \quad (3)$$

and where the product in the second term runs over particle indexes. This wavefunction also fulfils quantum symmetry requirements and is well suited for DMC purposes; however, it does not account for accurate description of quantum solids. We observe that when Ψ_{LNJ} is used for importance sampling, solid order is not preserved but instead glassy-like configurations are generated in the simulations [12]. In fact, substantially better variational energies are obtained in 2D solid hydrogen when using trial wavefunction Ψ_{SNJ} instead of Ψ_{LNJ} (see table I in [12]). Similar variational outcomes are also found in 2D solid ^{4}He. For instance, at density $\rho = 0.525 \, \sigma^{-2}$ ($\sigma = 2.556$ Å) we obtain $E/N^{\text{SNJ}} = 2.64(4)$ K ($b = 1.1 \, \sigma$ and $a = 7.5 \, \sigma^{-2}$, see section 3.1) whereas $E/N^{\text{LNJ}} = 4.49(15)$ K ($b = 1.3 \, \sigma$, $a = 7.5 \, \sigma^{-2}$ and $c = 4.0$, c appearing in the exponent of the McMillan factor, see section 3.1).

The poor variational quality of wavefunction Ψ_{LNJ} can be understood in terms of the localization factor which, contrarily to what is required to keep solid order, does not penalize multiple occupancy of the same site. By multiple occupancy of the same site here we mean a large probability of two particles near the same site getting too close to one another (that is as would be allowed by the Jastrow factor alone). Differences between trial wavefunctions Ψ_{SNJ} and Ψ_{LNJ} can be illustrated by a simple example of two particles in a one-dimensional (1D) lattice. For the sake of simplicity, we assume the distance between the atomic equilibrium positions to be one, the parameter in the Gaussian factors $(g(r))$ $a = 1/2$ (in arbitrary units) and switch off the Jastrow factor. The value of the square of wavefunctions Ψ_{SNJ} and Ψ_{LNJ}, $|\Psi_{\text{sol}}|^2$, in the case of pinning one of the particles in one lattice site (at $x = 0$) and then moving the second particle towards it, is plotted in figure 1. As one observes in there, the value of Ψ_{LNJ} at points $x = 1$ and 0 (which correspond to particles placed over different sites and particles placed over the same position, respectively) is identical, whereas $\Psi_{\text{SNJ}}(x = 1) > \Psi_{\text{SNJ}}(x = 0)$. Moreover, in the event of atomic overlap ($x = 0$) the drift force $1/\Psi(\partial\Psi/\partial x)$ corresponding to wavefunction Ψ_{SNJ} is much more repulsive than that of wavefunction Ψ_{LNJ}. In fact, the curve obtained in the Ψ_{LNJ} case resembles that of a liquid where the localizing factor can be thought of as a constant. Also it must be noted that the value of Ψ_{LNJ} is maximum at half way between 0 and 1, thus it will promote larger diffusion of the atoms throughout the volume.

A symmetrized trial wavefunction that has been successfully applied to the study of solid ^{4}He is the shadow wavefunction (SWF), proposed by Reatto *et al* more than 20 years ago [26, 27]. In the SWF formalism, an array of subsidiary particles (shadow particles) is defined and made to interact with the real atoms of the system; shadow particles are correlated among them and their coordinates are integrated
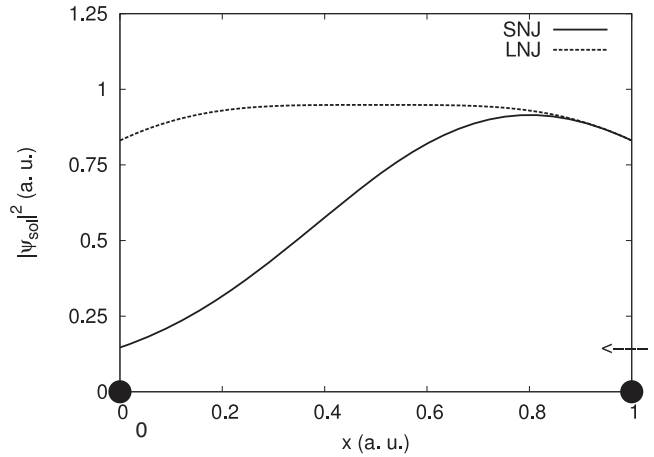

Figure 1. $|\Psi_{\text{LNJ}}|^2$ and $|\Psi_{\text{SNJ}}|^2$ (Jastrow factor equal to unity) functions in the simple case of two particles moving in one dimension and with lattice sites separated by one arbitrary unity.

over the whole volume in such a way that bosonic symmetry requirements are fulfilled by construction. At the variational level the SWF has been shown to provide a very accurate description of solid and liquid helium. Nevertheless, this kind of trial wavefunction has never been used for importance sampling in a DMC calculation. In spite of this, very recently the SWF has been implemented within the path integral ground-state (PIGS) formalism so that variational constraints, in principle, have been removed. This formalism has been used to explore solid ^{4}He in two dimensions [20] and we will comment on those results in section 3.2.

3. Results

3.1. 2D solid ^{4}He

DMC simulations of 2D solid ^{4}He in the triangular lattice configuration have been carried out for $N = 120$ particles in a (x, y) box where periodic boundary conditions are applied. Correlation functions in equation (2) are chosen to be of McMillan, $f(r) = \exp[-1/2(b/r)^5]$, and Gaussian, $g(r) = \exp[-1/2(ar^2)]$, form. Parameters b and a in factors $f(r)$ and $g(r)$ have been optimized using variational Monte Carlo (VMC) at a density of $\rho = 0.480 \, \sigma^{-2}$ ($\sigma = 2.556$ Å), and we obtain $b = 1.1 \, \sigma$ and $a = 7.5 \, \sigma^{-2}$ as best values (we neglect their weak dependence on density). Size effects have been corrected by assuming that atoms distribute uniformly beyond half the length of the simulation box. Wavefunction Ψ_{SNJ} already provides a good description of 2D solid ^{4}He at the variational level; for instance, at density $\rho = 0.550 \, \sigma^{-2}$ we obtain a variational total energy per atom E/N of 3.29(3) K which must compared with the SWF result [19] and variational benchmark $E/N^{\text{SWF}} = 3.10(1)$ K, and the Nosanow–Jastrow result $E/N^{\text{NJ}} = 3.18(2)$ K.

In figure 2, we plot DMC results for the total energy per particle E/N as a function of density in solid and liquid ^{4}He. Results for the liquid phase are taken from [28]. Previous Green's function Monte Carlo (GFMC) estimations obtained with a slightly different atomic pairwise interaction than used
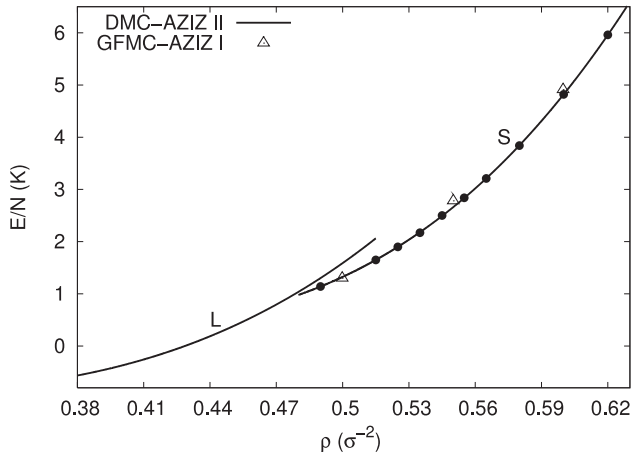
Figure 2. Energy per particle E/N of solid (S) and liquid (L) ^{4}He in two dimensions and zero temperature. Previous GFMC calculations [17] obtained with the Aziz I pair potential are shown for comparison (triangles). Results for the liquid phase are from [28].
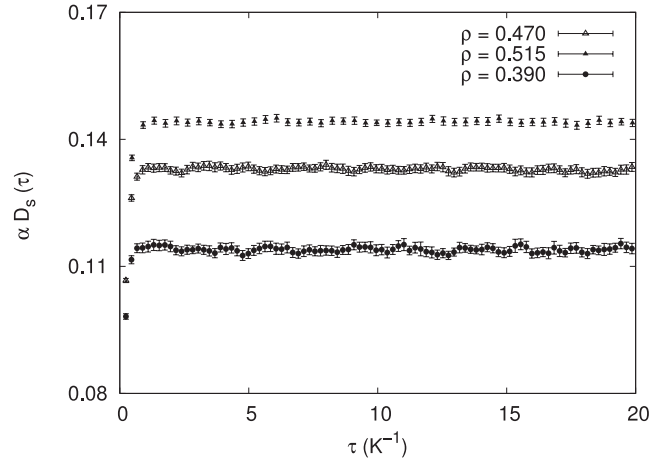

Figure 3. Diffusion of the center of mass of 2D solid ^{4}He in imaginary time calculated at a series of densities near, below and above the melting point. A small upwards shift has been applied to the curves calculated at higher densities in order to appreciate details of their slope.

here (referred to as Aziz I) [29] are included in the plot for comparison [17]. In the solid phase, we fit our total energy per atom results to the polynomial curve $E/N = e_0 + a\rho + b\rho^2 + c\rho^3$ with $e_0 = -9.28(0.6)$ K, $a = 87.41(3.4)$ Kσ^2, $b = -261.87(6.1)$ Kσ^4 and $c = 258.91(3.7)$ Kσ^6, the set of parameters which best reproduces them (statistical uncertainties of the fit are expressed within the parentheses). Once the energy function $E(\rho)$ is known in the liquid and solid phases, the corresponding melting and freezing densities, namely ρ_l and ρ_s, can be estimated by means of the double-tangent Maxwell construction. As a result, we obtain $\rho_l = 0.492 \, \sigma^{-2}$ and $\rho_s = 0.456 \, \sigma^{-2}$ which lie in between previous GFMC [17] ($\rho_l^{\text{GFMC}} = 0.471 \, \sigma^{-2}$, $\rho_s^{\text{GFMC}} = 0.443 \, \sigma^{-2}$) and variational SWF [19] ($\rho_l^{\text{SWF}} = 0.522 \, \sigma^{-2}$, $\rho_s^{\text{SWF}} = 0.475 \, \sigma^{-2}$) estimations. The small discrepancy with respect to the GFMC results can be understood in terms of the small differences in the atomic pairwise potential used. For instance, it is well known that the Aziz II potential provides atomic total energy values around 0.1 K smaller than the Aziz I potential does [28].

A well-known drawback of the NJ model (equation (1)) is the impossibility of answering the fundamental question of whether off-diagonal long range order (ODLRO) and/or superfluid behavior may be manifest or not in quantum solids. The SNJ model (equation (2)) correctly fulfils the Bose–Einstein statistics and provides that information to some extent. Quantitatively, ODLRO is measured by the condensate fraction n_0, which is estimated through the asymptotic behavior of the one-body density matrix $\rho(r)/\rho$, namely $n_0 = \lim_{r \to \infty} \rho(r)/\rho$. The one-body matrix is an operator which is non-diagonal in coordinate space and does not commute with the Hamiltonian H ($[H, \hat{\rho}] \neq 0$) so that DMC output for n_0 is a mixed estimator, though bias stemming from the trial wavefunction can be reduced significantly by means of extrapolated estimator techniques [11, 12].

Vitali *et al* [20] have recently adapted the PIGS formalism to the symmetrized SWF to investigate strictly 2D solid ^{4}He with it. Interestingly, the authors of this work conclude with the non-existence of ODLRO in perfect 2D solid ^{4}He. We will

comment on this finding in the next paragraph in the light of our ρ_s/ρ results.

Differently to the estimation of n_0, the superfluid density of a bosonic system can be calculated exactly using DMC (whereas this has not been possible yet within the PIGS method) by extending the winding-number technique, originally developed for PIMC calculations, to zero temperature [30]. Specifically, the expression for the superfluid fraction reads

$$\frac{\rho_s}{\rho} = \lim_{\tau \to \infty} \alpha \left(\frac{D_s(\tau)}{\tau} \right), \qquad (4)$$

where $\alpha = N/4D_0$ (2D case) with $D_0 = \hbar^2/2m$, $D_s(\tau) = \langle (\mathbf{R}_{\text{CM}}(\tau) - \mathbf{R}_{\text{CM}}(0))^2 \rangle$ and $\mathbf{R}_{\text{CM}}$ is the center of mass of the particles in the plane. In figure 3, we plot the function $D_s(\tau)$ calculated in the solid film at three different densities located near, above and below the corresponding freezing density. According to equation (4), the superfluid fraction ρ_s/ρ can be estimated directly from the slope of $D_s(\tau)$ at large imaginary time. In all the studied cases we find that the superfluid fraction of perfect 2D solid ^{4}He is vanishingly small, or to be more exact, it lies below our numerical threshold of $\sim 10^{-5}$. We found analogous ρ_s/ρ results in the perfect three-dimensional case [11]. As noted before, Vitali *et al* [20] have recently studied perfect 2D solid ^{4}He and concluded with the non-existence of ODLRO in this system.

Very recently, we have studied strictly 2D solid H$_2$ at zero temperature with analogous approaches to the one used here [12]. In 2D molecular hydrogen, we found that in the regime of very low densities (negative pressure regime, $\rho_{\text{H}_2} < 0.390 \, \sigma^{-2}$) a finite superfluid fraction appears in the crystal. Motivated by this result, and to understand the relation between normal and superfluid densities, we have carried out analogous calculations in 2D solid helium at stable and metastable conditions (that is at densities above and below $\rho_l = 0.492 \, \sigma^{-2}$, respectively). It is worth noticing that the

DMC method has already been used to study ground-state properties of metastable liquid ^{4}He (overpressurized) [31]. In the present case, we find a null value of ρ_s/ρ for any density down to $\rho = 0.390\ \sigma^{-2}$ (see figure 3). This result seems to be at odds with our previous findings in H$_2$ since solid helium possesses a larger degree of 'quantumness' compared to solid hydrogen. A possible explanation for this is that the density $\rho = 0.390\ \sigma^{-2}$ is still far from the spinodal point of 2D solid helium. In fact, ^{4}He is more compressible than H$_2$ (that is $|\partial P/\partial V|_{\text{He}} < |\partial P/\partial V|_{\text{H}_2}$) so it is likely that the critical density at which mechanical instabilities appear in the first system is below that of the second. Also it must be noted that very dilute solid helium films are far from being realizable since the liquid phase is always energetically more favorable at densities below $\rho = 0.480\ \sigma^{-2}$ (contrarily to what occurs in 2D H$_2$). In order to complete our study of low-dimensional solid helium we have explored a system which can be considered as somewhat more realistic, namely a quasi-2D film.

3.2. Quasi-2D solid ^{4}He

Very recent torsional-oscillator-like experiments performed in the second layer of solid ^{4}He adsorbed on graphite seem to point towards the possible existence of a new kind of supersolid phase [32]. Physical quantities such as the density of particles, temperature and degree of corrugation with the substrate, appear to have an important effect on the value of this supersolid-like signal. Aimed at investigating the origins of this low-dimensional supersolidity, which is totally absent in strictly 2D solid ^{4}He, we have studied an interesting kind of simple model: a quasi-2D film. In this work, a quasi-2D solid refers to a system of interacting ^{4}He particles with atomic displacements mostly confined to a plane but which can spread over the z-axis due to zero-point oscillations (see figure 4). This model grasps some essential features of helium layers adsorbed on carbon-based surfaces like graphene and graphite and could be relevant to describing surface effects in bulk crystals. There are several advantages in exploring this model system instead of performing more realistic simulations of helium films adsorbed on carbon-based surfaces [13–16]. First is the reduction of computational cost which derives from ignoring explicit interactions with the substrate and that allows us to explore the superfluid properties of the model under a wide range of conditions. Second, confinement in the z-direction can be tuned at will in order to explore the relation between the superfluid fraction ρ_s/ρ and the magnitude of the spatial out-plane fluctuations $\langle \Delta z^2 \rangle = \langle (z - \langle z \rangle)^2 \rangle$, which are related to the strength of the helium film interactions with the substrate. Certainly, realistic simulations of ^{4}He films are necessary to fully understand the origins of supersolid manifestations; however, here we assume simplified interatomic interactions and atomic structure (only the triangular lattice is considered) in exchange for analyzing possible effects derived from the density of particles and strength of the film–substrate interactions. The density range in which we concentrate corresponds to that of an incomplete first layer of solid helium adsorbed on graphite
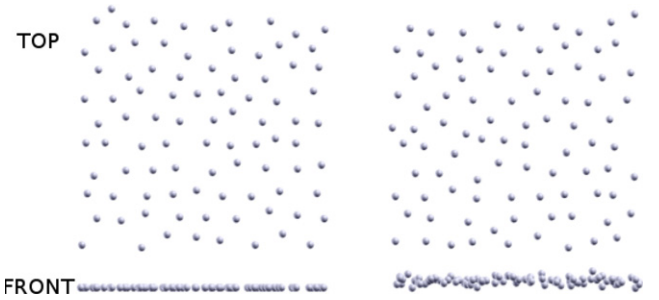

Figure 4. Top and front views of strictly two-dimensional (left) and quasi-2D (right) solid ^{4}He at density $\rho = 0.515\ \sigma^{-2}$ and zero temperature.

(that is $0.416 < \rho < 0.745$ atom/σ^3) [16], so the effects relating to the promotion of atoms to second or higher layers are not considered.

Local fluctuations of the atomic positions in the z-direction are achieved by imposing an external out-of-plane harmonic potential trap $V_c(z) \propto (z - z_0)^2$, where z_0 is the equilibrium position of the film in that direction. The Hamiltonian describing the quasi-2D system then is $H = T + V_{\text{Aziz II}} + V_c$. The symmetrized trial wavefunction that we use to describe the quasi-2D system is

$$\Psi_{\text{SNJ}}^{\text{q}-2\text{D}}(\mathbf{r}_1, \ldots, \mathbf{r}_N) = \prod_{i<j}^N f(r_{ij}) \prod_{J=1}^N \left(\sum_{i=1}^N g(r_{iJ}^{xy}) \right)$$
$$\times \prod_{i=1}^N \exp\left(-\tfrac{1}{2}\chi z_i^2\right) \tag{5}$$

where r_{iJ}^{xy} is the projection of the vector $\mathbf{r_i} - \mathbf{R_J}$ over the xy-plane, lattice vectors being $\{\mathbf{R_J} = (a, b, 0)\}$, and the value of parameter χ is explicitly related to the value of the atomic spatial z-fluctuation by $\langle \Delta z^2 \rangle = 1/2\chi$. The trial wavefunction $\Psi_{\text{SNJ}}^{\text{q}-2\text{D}}$ is equivalent to Ψ_{SNJ} in equation (2) but with additional Gaussian localizing factors on the z-direction; these localizing functions correspond to the exact Schrödinger equation solution of a particle moving under the action of the harmonic potential field V_c. Since the computational technique used in this section is the DMC method and the magnitude of the atomic z-spatial fluctuations analyzed is fairly small, we have not attempted to construct explicit z-pairwise correlations on the trial wavefunction. It must be noted that these correlations are implicitly taken into account by the Jastrow factor contained in $\Psi_{\text{SNJ}}^{\text{q}-2\text{D}}$. Variational parameters contained in expression (5) are set to the same value as used in the study of strictly 2D solid ^{4}He, with the exception of χ which is varied according to the value of the spring constant corresponding to the harmonic trap.

Next, we comment on the superfluid fraction results obtained at several densities and z-confinement conditions. In table 1, we report the dependence of the estimated superfluid density fraction on the density of particles and the z-coordinate fluctuation $\langle \Delta z^2 \rangle$; in figure 5 we also show the evolution of function $D_s(\tau)$ on imaginary time at density $\rho = 0.470\ \sigma^{-2}$ and several atomic z-confinements. It is found that in the $\langle \Delta z^2 \rangle^{1/2} \leqslant 0.08\ \sigma$ cases (not shown) the superfluid density
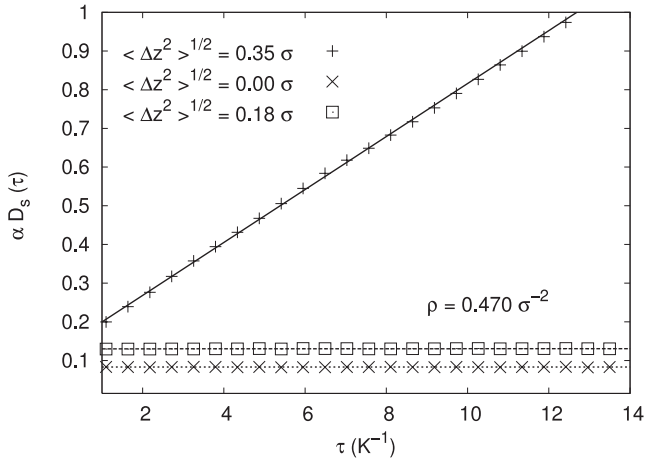
Figure 5. Diffusion of the center of mass of quasi-2D solid ^{4}He calculated at the density $\rho = 0.470\,\sigma^{-2}$ and different values of the atomic z-spatial fluctuations $\langle\Delta z^2\rangle$.

Table 1. Calculated superfluid fraction (expressed in %) of quasi-2D solid ^{4}He as a function of the density of particles and atomic spatial z-fluctuation $\langle\Delta z^2\rangle$.

ρ (σ^{-2})	$\langle\Delta z^2\rangle^{\frac{1}{2}}$ (σ)		
	0.18	0.22	0.35
0.470	0.003(1)	0.16(1)	6.85(1)
0.515	0.015(1)	0.010(1)	17.27(1)
0.600	0.0	0.009(1)	54.21(1)

is always vanishing, which turns out to be consistent with what is found in the strictly 2D case. On the contrary, when confinement in the z-direction is shallow, that is the case where $\langle\Delta z^2\rangle^{1/2} = 0.35\,\sigma$, the value of ρ_s/ρ is always large and increases as the density of particles is raised (see table 1). Results in the last column of table 1 appear to show a competition between in-plane and out-plane interactions; as the system is compressed, in-plane repulsive interactions become progressively more important so that atoms prefer to spread over the z-direction wherein potential confinement is mild and they can move more freely. This has the overall effect of enhancing the superfluid response of the system. In the $\langle\Delta z^2\rangle^{1/2} = 0.18$ and $0.22\,\sigma$ cases, estimated ρ_s/ρ trends on density are not that monotonic. At $\langle\Delta z^2\rangle^{1/2} = 0.18\,\sigma$, we see that ρ_s/ρ first increases when the density of particles is raised whereas next it diminishes down to zero value under further compression of the system. This behavior can be understood in terms of the imposed z-axis confinement and atomic in-plane interactions as well. When the density of particles is first increased, atoms minimize their potential energy by spanning over the z-axis in order to keep a distance from their neighbors and move as freely as possible. The total space available for the atoms then becomes larger so the effective density of the system becomes smaller. The value of ρ_s/ρ consequently increases. However, when density is further raised, out-plane atomic excursions are not favorable any more because large displacements along the z-direction require too much energy. The value of ρ_s/ρ then decreases because atomic motion is
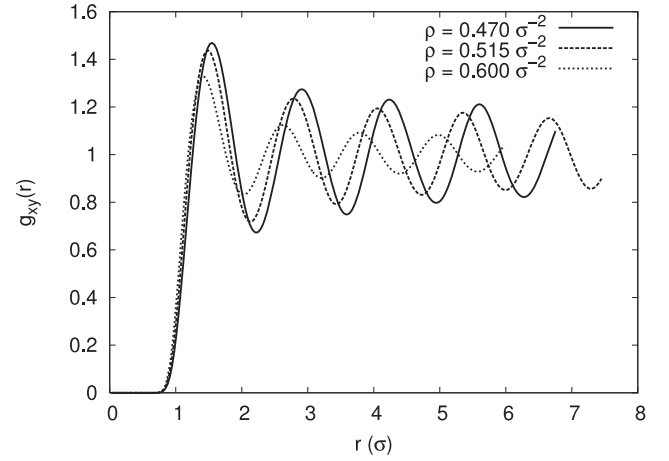

Figure 6. Radial pair-distribution function calculated on the xy-plane of the quasi-2D film at different densities and fixed amplitude of z-fluctuations $\langle\Delta z^2\rangle^{1/2} = 0.35\,\sigma$. At density $\rho = 0.600\,\sigma^{-2}$, the peaks and valleys of the $g_{xy}(r)$ function turn out to be appreciably less pronounced than in the other cases considered.

tightly bound to the xy-plane and the effective density of the system becomes large. The competition between in- and out-plane interactions as modulated by the density of particles is responsible for the enhancement/depletion of the observed superfluid response of the system. At z-axis confinement $\langle\Delta z^2\rangle^{1/2} = 0.22\,\sigma$, the trend of ρ_s/ρ with density exhibits an intermediate behavior between that found in the 0.18 and $0.35\,\sigma$ cases.

Regarding the stability of the quasi-2D solid film, we note that in all the studied cases crystal-like order has been found as witnessed by (i) the marked oscillating shape of the radial pair-distribution functions $g_{xy}(r)$ obtained considering the projection of the atomic positions on the xy-plane (see figure 6), and (ii) the peaked pattern of the corresponding radial averaged structure factors S_{xy} that scale with the number of atoms (see figure 7). Nevertheless, in the $\langle\Delta z^2\rangle^{1/2} = 0.35\,\sigma$ cases the film is likely to be a kind of glass system since the values of the corresponding maximum $S_{xy}(k)$ peaks are small (see figure 7, lower panel) and the ρ_s/ρ values obtained are quite large (last column in table 1) in comparison to the results obtained upon tighter z-confinement. In fact, large superfluid fractions ($\sim$10–60%) have been estimated in metastable ^{4}He glass systems using the PIMC method [9]. Moreover, we have calculated the total energy of a quasi-2D liquid system at the same density and $\langle\Delta z^2\rangle^{1/2}$ conditions as in the quasi-2D solid system, using a Jastrow factor and Gaussian z-localizing factors as importance sampling. It is found that in all the $\langle\Delta z^2\rangle^{1/2} = 0.35\,\sigma$ cases the quasi-2D solid film is metastable (that is $E_J^{q-2D} < E_{SNJ}^{q-2D}$) whereas it is stable in the rest of $\langle\Delta z^2\rangle^{1/2}$ and ρ cases (that is $E_{SNJ}^{q-2D} < E_J^{q-2D}$). For instance, at $\langle\Delta z^2\rangle^{1/2} = 0.35\,\sigma$ and $\rho = 0.515\,\sigma^{-2}$ we obtain $E_J^{q-2D} = 2.71(2)$ K/atom and $E_{SNJ}^{q-2D} = 3.66(2)$ K/atom, while at $\langle\Delta z^2\rangle^{1/2} = 0.18\,\sigma$ and the same density we obtain $E_J^{q-2D} = 16.29(3)$ K/atom and $E_{SNJ}^{q-2D} = 15.81(2)$ K/atom. This last outcome, in analogy with the 3D case, appears to corroborate the hypothesis that the results obtained at
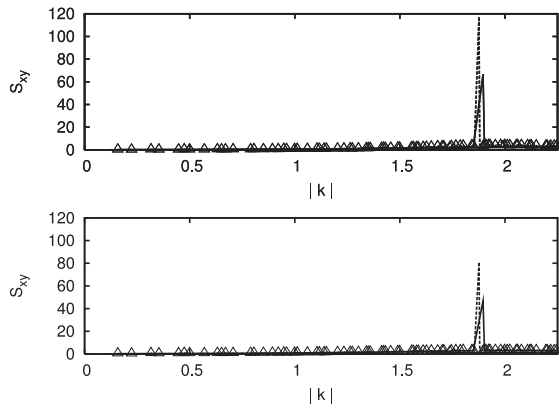
Figure 7. Calculated radial averaged structure factor $S_{xy}(k)$ of the quasi-2D solid film at $\rho = 0.515\ \sigma^{-2}$ (k is in units of σ^{-1}). Solid lines represent calculations performed with $N = 120$ atoms, dashed lines calculations performed with $N = 224$ atoms and triangles correspond to results obtained for a quasi-2D liquid system ($N = 120$ atoms). In the lower and upper panels, we show results obtained for z-confinement $\langle \Delta z^2 \rangle^{1/2} = 0.35\ \sigma$ and $\langle \Delta z^2 \rangle^{1/2} = 0.22\ \sigma$, respectively.

Figure 8. Calculated atomic z-density profile (solid line) in the quasi-2D solid system at $\rho = 0.470\ \sigma^{-2}$ and $\langle \Delta z^2 \rangle^{1/2} = 0.18\ \sigma$. For comparison, we plot the corresponding normalized Gaussian z-localizing factor ($\chi = 16\ \sigma^{-2}$) entering trial wavefunction $\Psi_{\text{SNJ}}^{\text{q}-2\text{D}}$. The distance is in units of σ.

z-confinement $\langle \Delta z^2 \rangle^{1/2} = 0.35\ \sigma$ correspond to quasi-2D glass systems.

It is worth noticing that although particles in the quasi-2D film are allowed to move in the z-direction, there is not enough energy to excite the levels of the transverse confinement and the system is kinematically two-dimensional. The radial motion is frozen to zero-point oscillations and the magnitude of z-fluctuations therefore is related to the length $\langle \Delta z^2 \rangle^{1/2}$. We illustrate this in figure 8 where we plot the atomic z-density profile calculated in the quasi-2D solid film at $\rho = 0.470\ \sigma^{-2}$ and $\langle \Delta z^2 \rangle^{1/2} = 0.18\ \sigma$ using the pure estimators technique [23] and compare it with the corresponding normalized Gaussian z-localizing factor entering $\Psi_{\text{SNJ}}^{\text{q}-2\text{D}}$ (case $\chi = 16\ \sigma^{-2}$).

4. Conclusions

We have studied 2D and quasi-2D solid ^{4}He at zero temperature by means of the diffusion Monte Carlo method and using the recently proposed symmetrized trial wavefunction Ψ_{SNJ} as importance sampling. We have estimated the superfluid density fraction of 2D solid ^{4}He at $T = 0$ and found that is negligible down to a density of $\rho = 0.390\ \sigma^{-2}$. Importantly, by allowing the atoms to move along the z-axis, we observe the appearance of a superfluid response that coexists with the crystalline order of the system. The magnitude of this response is shown to depend on the degree of z-axis confinement and the density of particles. This finding is valuable for the realization and interpretation of more realistic simulations of helium layers adsorbed on carbon-based surfaces, where the interactions with the substrate must be taken into account accurately in order to make rigorous judgments about the existence of superfluidity and/or ODLRO. In view of the present results for the quasi-2D solid, it can be suggested that a well-suited system in which to observe a finite superfluid signal is the first layer of ^{4}He on top of
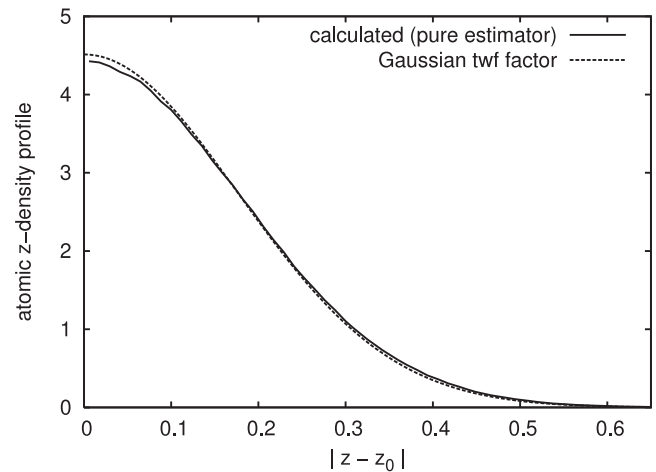
graphene or graphite [13] which stabilizes in a triangular lattice and possesses relatively small density. Work to verify this hypothesis is in progress.

References

[1] Cazorla C, Errandonea D and Sola E 2009 *Phys. Rev.* B **80** 064105
[2] Cazorla C and Boronat J 2008 *Phys. Rev.* B **77** 024310
[3] Kim E and Chan M H W 2004 *Science* **305** 1941
[4] Kim E and Chan M H W 2004 *Nature* **427** 225
[5] Balibar S and Caupin F 2008 *J. Phys.: Condens. Matter* **20** 173201
[6] Sasaki S, Ishiguro R, Caupin F, Harris H J and Balibar S 2006 *Science* **313** 1098
[7] Ceperley D M and Bernu B 2004 *Phys. Rev. Lett.* **93** 155303
[8] Clark B K and Ceperley D M 2006 *Phys. Rev. Lett.* **96** 105302
[9] Boninsegni M, Prokof'ev N and Svistunov B 2006 *Phys. Rev. Lett.* **96** 105301
[10] Boninsegni M, Kuklov A B, Pollet L, Prokof'ev N V, Svistunov B V and Troyer M 2007 *Phys. Rev. Lett.* **99** 035301
[11] Cazorla C, Astrakharchik G E, Casulleras J and Boronat J 2009 *New J. Phys.* **11** 013047
[12] Cazorla C and Boronat J 2008 *Phys. Rev.* B **78** 134509
[13] Gordillo M C and Boronat J 2009 *Phys. Rev. Lett.* **102** 085303
[14] Pierce M E and Manousakis E 1999 *Phys. Rev. Lett.* **83** 5314
[15] Greywall D S and Busch P A 1991 *Phys. Rev. Lett.* **67** 3535
[16] Corboz P, Boninsegni M, Pollet L and Troyer M 2008 *Phys. Rev.* B **78** 245414
[17] Whitlock P A, Chester G V and Kalos M H 1988 *Phys. Rev.* B **38** 2418

[18] Gordillo C and Ceperley D 1998 *Phys. Rev.* B **58** 6447
[19] Krishnamachari B and Chester G V 2000 *Phys. Rev.* B
     61 9677
[20] Vitali E, Rossi M, Tramonto F, Galli D E and Reatto L 2008
     Phys. Rev. B **77** 180505(R)
[21] Aziz R A, McCourt F R W and Wong C C K 1987 *Mol. Phys.*
     61 1487
[22] Boronat J and Casulleras J 1994 *Phys. Rev.* B **49** 8920
[23] Casulleras J and Boronat J 1995 *Phys. Rev.* B **52** 3654
[24] Cazorla C and Boronat J 2008 *J. Phys.: Condens. Matter*
     20 015223
[25] Zhai H and Wu Y-S 2005 *J. Stat. Mech.* P07003
[26] Vitiello S, Runge K and Kalos M H 1988 *Phys. Rev. Lett.*
     60 1970
[27] Reatto L and Masserini G L 1988 *Phys. Rev.* B **38** 4516
[28] Giorgini S, Boronat J and Casulleras J 1996 *Phys. Rev.* B
     54 6099
[29] Aziz R A, Nain V P S, Carley J S, Taylor W L and
     McGonville G T 1979 *J. Chem. Phys.* **70** 4330
[30] Zhang S, Kawashima N, Carlson J and Gubernatis J E 1995
     Phys. Rev. Lett. **74** 1500
[31] Vranješ L, Boronat J, Casulleras J and Cazorla C 2005 *Phys.
     Rev. Lett.* **95** 145302
[32] Nyéki J and Saunders J 2009 *APS March Mtg*